 AIAA 2013-1765

Modelling of Fiber/Matrix Debonding of Composites under Cyclic Loading

Paria Naghipour[1]
Ohio Aerospace Institute, 22800 Cedar Point Road, Brookpark, OH 44142

Evan J. Pineda[2], Brett A. Bednarcyk[3], Steven M. Arnold[4]
NASA Glenn Research Center, 21000 Brookpark Road, Cleveland, OH 44135

Abstract

The micromechanics theory, generalized method of cells (GMC), was employed to simulate the debonding of fiber/matrix interfaces, within a repeating unit cell subjected to global, cyclic loading, utilizing a cyclic crack growth law. Cycle dependent, interfacial debonding was implemented as a new module to the available GMC formulation. The degradation of interfacial stresses, with applied load cycles, was achieved via progressive evolution of the interfacial compliance. A periodic repeating unit cell, representing the fiber/matrix architecture of a composite, was subjected to combined normal and shear loadings, and degradation of the global transverse stress in successive cycles was monitored. The obtained results were compared to values from a corresponding finite element model. Reasonable agreement was achieved for combined normal and shear loading conditions, with minimal variation for pure loading cases. The local effects of interfacial debonding, and fatigue damage will later be combined as sub-models to predict the experimentally obtained fatigue life of Ti-15-3/Sic composites at the laminate level.

I. Introduction

Advanced multi-phase composites continue to be one of the leading materials in the aerospace research and design community. One main challenge related to composites involves the development of accurate material and structural design and analysis tools. With titanium matrix composites (TMCs), debonding at the interface of the fiber and matrix is a main characteristic. Furthermore, residual stresses arising from inelastic and time/history dependent deformation of the titanium matrices– even during manufacturing have a major impact on the behavior of TMCs. The challenging fact is that most of these phenomena are not directly measurable and interact with each other during the whole failure process of the TMC. Therefore, advance analytical approaches are needed to account for the characteristics of TMCs described above.

The approach taken herein employs a micromechanics model known as the generalized method of cells (GMC) [1,2]. This model is analytical in nature and its formulation involves application of several governing conditions in an average sense[3]. Because of this averaging and due to a decoupling between normal and shear field components, the model seems to be less accurate than traditional finite element analysis (FEA) at the micro scale, but makes it many times more efficient computationally. Furthermore, FEA based approaches often require complex boundary conditions to be applied to the unit cell, which can make applying different types of loading combinations cumbersome. The large number of elements required for FEA analysis of the unit cell, makes this method intractable is the composite being analyzed is part of a larger structural problem. Moreover, GMC provides the local fields in composite materials, allowing incorporation of arbitrary inelastic constitutive models for the composite phases as well as other micro scale effects such as fatigue damage, fiber breakage, and fiber-matrix debonding. Finally, it results in closed-form constitutive equations for the composite, which, combined

[1] Research Associate, Ohio Aerospace Institute, 22800 Cedar Point Road, Brookpark, OH 44142
[2] NASA Research Engineer, Mechanics and Life Predictions Branch, 21000 Brookpark Rd., AIAA member
[3] NASA Research Engineer, Mechanics and Life Predictions Branch, 21000 Brookpark Rd., AIAA Associate Fellow
[4] Branch Chief,, Mechanics and Life Predictions Branch, 21000 Brookpark Rd., AIAA senior member

with its efficiency, makes the model ideal for inclusion within larger structural analysis approaches to simulate the composite behavior at a material point.

In this investigation, the composites under consideration are Carbon/epoxy and silicon carbide/titanium (SiC/Ti) composites. Previously, GMC had been employed by Bednarcyk and Arnold [4], to simulate the tensile deformation, failure, and low cycle fatigue (LCF) life of unidirectional SCS-6/Ti-15-3, as well as SCS-6/Ti-15-3 laminates. Bednarcyk and Arnold [4], modeled the inelastic behavior of the Ti-15-3 using incremental (time-independent) plasticity theory, utilizing local (micro scale) models for longitudinal fiber breakage [5], fiber-matrix debonding [6], and fatigue damage [7]. The interfacial (fiber/matrix) debonding was controlled using an Evolving Compliant Interface (ECI), which related the evolution of the interfacial traction to time, explicitly. The major focus of this paper is simulation of the cyclic debonding of the same material system utilizing an implicit, Paris-type cyclic crack/debonding growth law (instead of the ECI model), and linking it to the mentioned sub-models. During cyclic debonding, a distinction needs to be made between the loading and unloading paths allowing for hysteresis. This physical phenomenon is represented mathematically by incorporating the successive evolution of the debonding compliance with number of cycles (with the help of Paris-type cyclic crack/debonding growth law). The Paris-type fatigue debonding law has been successfully implemented by Naghipour et al. [8] within the context of FE cohesive zone formulation to simulate the inter-laminar delamination of composites.

II. Constituent Response

The micromechanics model employed to simulate the response of the SiC/Ti-15-3 composite is the generalized method of cells (GMC) developed by Aboudi [1,2]. The geometry of the doubly periodic version of GMC is shown in Figure. 1, wherein the microstructure of a periodic material is represented by a rectangular repeating unit cell consisting of an arbitrary number of rectangular subcells, each of which may be a distinct material. The methodology of GMC and its reformulation to be embedded with classical laminate theory is described thoroughly by Aboudi [1,2] and Bednarcyk and Arnold [4].

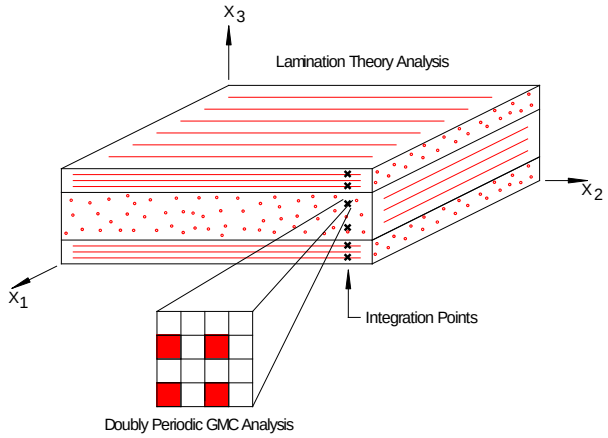

Figure. 1: Schematic showing the lamination theory geometry with GMC embedded to represent the behavior of the composite material at the through-thickness integration points.

The composite material examined by Bednarcyk and Arnold [4], which will be used in this study as well, consists of a Ti-15-3 matrix reinforced by continuous SCS-6 silicon carbide fibers. As a start point, incorporating sub-models for the behavior of the individual phases, the SCS-6 fiber was treated as an elastic, isotropic material with the temperature-dependent properties as specified by Bednarcyk and Arnold [4], and the elastoplastic constitutive response of the Ti-15-3 matrix was modeled using Mendelson's [9] time-independent incremental plasticity theory. This theory provides the inelastic strain increment for an isotropic material (with some manipulation of Mendelson's [9]equations) and adding the temperature dependency as described by Bednarcyk and [4],

$$d\varepsilon_{ij}^{in} = \left(1 - \frac{\bar{\sigma}_{eff}}{3G\varepsilon_{st}}\right) e_{ij}^{'} \tag{1}$$

where G is the elastic shear modulus, ε_{st} is the equivalent modified total strain deviator, and $e`_{ij}$ are the components of the modified total strain deviator (see Mendelson [8] and Bednarcyk and Arnold [4] for details).

III. Fiber Breakage and Interfacial Debonding of SiC/Ti-15-3 under Quasi-Static and Cyclic Loading

The breakage of individual fibers causing the overall failure of longitudinally loaded unidirectional SiC/Ti composites was successfully addressed via a sub-model in Bednarcyk and Arnold [4] utilizing Curtin's [5] effective fiber breakage model within GMC context. Using fiber strength statistics combined with a shear-lag analysis, Curtin [5] developed a general equation describing the stiffness degradation of an effective fiber that represents all fibers in the composite as the composite is loaded longitudinally. The effective fiber elastic modulus is given by Equation (2),

$$E_f^* = \frac{1}{2}\left(1+\exp\left(-\left[\frac{E_f \varepsilon_f^{mech}}{\sigma_c}\right]^{m+1}\right)\right)E_f \tag{2}$$

E_f is the original fiber modulus, ε_f^{mech} is the fiber longitudinal mechanical strain, m is the fiber Weibull modulus, and σ_c is an empirically obtained stress value defined explicitly by Curtin [5] Bednarcyk and Arnold [4] compared the longitudinal tensile deformation and failure of SCS-6/Ti-15-3 composites , employing a simple 2×2 GMC repeating cell containing a single fiber, as the Curtin model represents the behavior of all fibers within the composite as one effective fiber. Although some under predictions are observed in lower temperatures for three different fiber volume fractions, the model still does a reasonably good job of predicting the composite ultimate tensile strength (UTS) for these three cases (see Bednarcyk and Arnold [4]).

It is well known that unidirectional SiC/Ti composites exhibit fiber-matrix debonding when subjected to off-axis loading (see Johnson et al. [10], Mall and Nicholas [11], and Bednarcyk and Arnold [12]). A model for quasi-static interfacial debonding known as the evolving compliant interface (ECI) model was developed and implemented within GMC by Bednarcyk and Arnold [12], and further used to successfully model the interfacial debonding behavior in SCS-6/Ti-15-3 in Bednarcyk and Arnold [4]. The debonding methodology of GMC employs the concept of a flexible interface (Jones and Whittier [13]), wherein a discontinuity in the normal or tangential displacement component at an interface, I, is permitted. These discontinuities are taken to be proportional to the appropriate stress component at the interface such that,

$$\left[u_n\right]^I = R_n \sigma_n|^{\mathrm{I}} \qquad \sigma_n = \sigma^n{}_{DB} \tag{3}$$

$$\left[u_t\right]^I = R_t \sigma_t|^{\mathrm{I}} \qquad \sigma_t = \sigma^t{}_{DB} \tag{4}$$

$[u_n]^I$ and $[u_t]^I$ are the normal and tangential displacement discontinuities at the interface, with $\sigma_n|^I$ and $\sigma_t|^I$ as corresponding interfacial stresses, R_n and R_t are empirical debonding parameters representing the effective compliance of the interface, and σ^n_{DB}, σ^t_{DB} are the normal and tangential strengths of the interface.

The main focus of this paper is on developing a fatigue debonding model to be combined with the above-mentioned sub-models to thoroughly capture the ongoing failure mechanism under cyclic loading. This model utilizes a similar strategy to the ECI model described above with a compliance (R) definition evolving with number of cycles. The approach followed for defining the cyclically evolving compliance is based on linking damage and fracture mechanics in the GMC context. Embedding a cyclic fracture law, such as Paris law (Paris and Erdogan, (1963)), in to the debonding formulation enables us to set up a semi-physical base for the cyclic debonding model. As a start point the cyclic evolution equation can be written as:

$$\frac{\partial R}{\partial N} = \frac{\partial R}{\partial A}\frac{\partial A}{\partial N} \tag{5}$$

A represents the debonding area, and *dA/dN* is the growth rate of the damaged (debonded) area. Using chain rule, Equation (5) can be rewritten as:

$$\frac{\partial R}{\partial N} = \frac{\partial R}{\partial \sigma}\frac{\partial \sigma}{\partial A}\frac{\partial A}{\partial N} \tag{6}$$

The first part of Equation (6) (rate of change of compliance with the debonded area, *dR/dA*) can be calculated analytically if a linear descent is assumed for the debonding stress versus displacement (see Figure. 2 below)

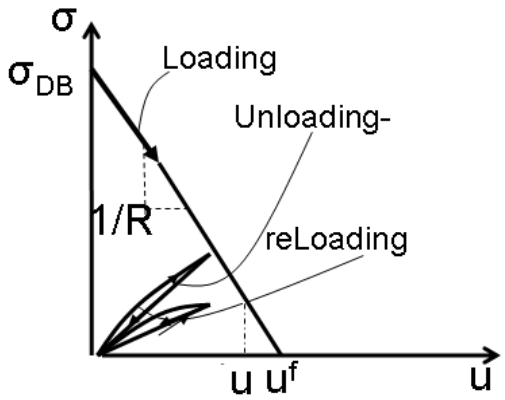

Figure. 2: Linear descent of the interfacial debonding (interfacial stress versus displacement)

A is the debonded area under Figure (2) from the initial debonding up to a specified displacement (*u*). The stress displacement equation (based on Figure.2) can be written as:

$$\sigma = \frac{-\sigma_c}{u_c}u + \sigma_c = \frac{-\sigma_c}{u_c}R\sigma + \sigma_c \tag{7}$$

Writing R in terms of the debonding stress gives:

$$R = \frac{\sigma - \sigma_c}{\frac{-\sigma\sigma_c}{u_c}} \tag{8}$$

The derivative of the compliance with respect to debonding stress *(dR/dσ)* reads:

$$\frac{\partial R}{\partial \sigma} = \frac{-u_c}{\sigma^2} \tag{9}$$

Considering Figure. 2, in order to define the debonded area in terms of debonding stress, one can write:

$$A = \frac{\sigma + \sigma_c}{2}u \tag{10}$$

Rewriting Equation (10) using Equation (7) gives:

$$A = \frac{\sigma + \sigma_c}{2}(\sigma - \sigma_c)\frac{-u_c}{\sigma_c} \tag{11}$$

Using Equation (11), the derivative of the debonding stress with respect to the debonding area is

$$\frac{\partial \sigma}{\partial A} = -\frac{\sigma_c}{\sigma u_c} \tag{12}$$

Substituting Equation (12) and (9) into the definition of *dR/dA* (Equation (5)), we obtain:

$$\frac{\partial R}{\partial A} = \frac{\sigma_c}{\sigma^3} \tag{13}$$

The second part of Equation (5), *dA/dN*, represents a Paris-type (Paris and Erdogan [14]) equation relating the cyclic growth of the debonding to strain energy release rate. This part incorporates a physical basis to the cyclic debonding formulation within the GMC context. In a degradation process involving cyclic loading, the debonded area grows as the number of cycles increases. It can be assumed that the increase in the cracked area is equivalent to the increase in the amount of debonded area, which is equal to the increase in the debonded area of all of the involved subcells. Therefore the crack growth rate in Paris-type law can be assumed to be equal to sum of the debonded area growth rates of all debonded subcells. Assuming a mean value for the debonded area growth rate ($\tilde{A}_{debonded}$) and assuming the mean area of the subcells does not change significantly (can be assumed as constant) the second part of Equation (5) can be rewritten as:

$$\frac{\partial A}{\partial N} = \sum \frac{\partial A_{debonded}}{\partial N} = m\frac{\partial \tilde{A}_{debonded}}{\partial N} \tag{14}$$

m is an averaging coefficient, which can be calibrated back from available experimental results. The debonding area growth rate in the present model (dA/dN), is approximated using the Paris-type law (Paris and Erdogan [14]), as:

$$\frac{\partial A}{\partial N} = mC^{Paris}\left(\frac{\Delta G}{G_c}\right)^{m^{Paris}} \tag{15}$$

C^{Paris}, m^{Paris}, and G_c are material parameters that depend on the failure mode (normal, shear or combination of both), and *G* is the strain energy release rate, which can be approximated as:

$$\Delta G = \sigma du \tag{16}$$

Substituting u=Rσ from Equation (2) in to Equation (16) and using the chain rule derivative, Equation (15) can be rewritten as:

$$\frac{\partial A}{\partial N} = mC^{Paris}\left(\frac{dR\sigma + Rd\sigma}{G_c}\right)^{m^{Paris}} \tag{17}$$

The compliance increment (*dR*), current compliance (*R*), stress (σ) and stress increment ($d\sigma$) are updated throughout GMC. However, an initial non-zero value must be assumed for the initial compliance increment. This is obtained based on Equation (5), assuming that at the beginning of debonding the strain energy release rate, *G*, is zero, but a threshold value (G_{th}) must exist for the fatigue debonding to start growing:

$$\left(\frac{\partial R}{\partial N}\right)_{initial} = C^{Paris}\left(\frac{G_{th}}{G_c}\right)^{m^{Paris}} \tag{18}$$

No debonding is observed if the strain energy release rate is smaller than the fatigue threshold of the strain energy release rate, and the value for G_{th} can be calibrated using the Paris-plot (Paris and Erdogan [14]) after cyclic experiments. In the GMC context, this threshold value will be approximated from the micro-level matrix-matrix damage sub-model.

Although assuming a cycle-by-cycle analysis ($\Delta N=1$), provides the most accurate results, in a failure process involving high cycle fatigue, it might become computationally intractable. Therefore, a cycle jump strategy is supposed to be further formulated for the cyclic debonding module, to work parallel with the ECI sub-model in case of high-cycle fatigue. The method would be based on *dR* incrementation to set a limit value for the maximum number of the cycles to be jumped.

IV. Results and Discussion

In order to verify the newly implemented cyclic debonding module, a one-to-one comparison of a debonding single subcell with an analogous element finite element simulation is carried out, and the results are presented in Figure. 3. A single epoxy subcell is subjected to strain driven cyclic loading, and the interfacial debonding and stress degradation are monitored as number of cycles grow. The FE model, consisting of two epoxy elements with a single cohesive element between them to capture the cyclic interfacial debonding, is. The user-developed cohesive element has been proved to have a reliable predictive capability of capturing the cyclic delamination growth according to Naghipour et al. [8], and therefore is used as the first verification step here. A very good agreement of interfacial stress degradation in subsequent cycles is achieved, when comparing single-cell GMC with the one-element FE simulation. The same parameter set, obtained partially from available sources in literature or data calibration, is used for GMC and the FE simulation (Table. 1).

Mechanical properties of epoxy 8552			
E_{11} (MPa)	ν_{12}	G_{12} (MPa)	
3450	0.35	1270	
Properties of interface (UEL and GMC) C^{Paris} =0.0616 mm/cycle m^{Paris} =1.15 G_{th}= 0.001 mJ/ mm^2 ΔN=1 m=1			
Nromal strength (MPa) Only UEL	Shear Strength (MPa) Only UEL	Initial Stiffness (N/mm) Only UEL	Total G_c (mJ/mm^2) GMC and UEL
75	80	10^7	0.8

Table.1: Parameter set for the one element verification test (GMC versus FE simulation)

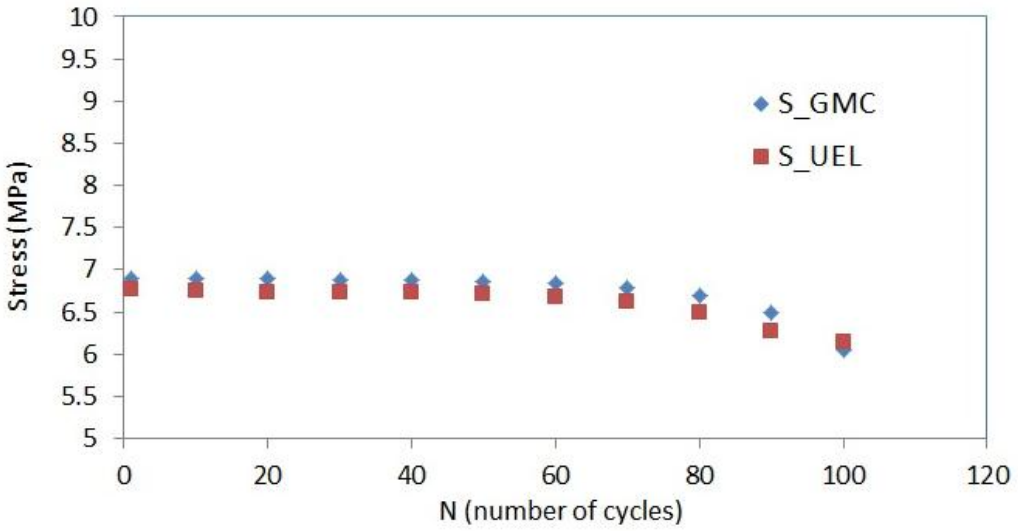

Figure. 3: Interfacial debonding stress degradation versus number of cycles (epoxy subcell)

In order to numerically validate the predictive capability of the newly implemented cyclic debonding module in GMC, a one to one comparison to analogous finite element simulations was carried out as a second case study. The successive degradation in the global transverse stress, caused by interfacial fatigue debonding of the fiber/matrix, was compared for corresponding GMC and FEM simulations. Pure normal, pure shear and various mixed mode (normal plus shear) loadings were applied to verify the accuracy of the model, under combined effects of normal and shear loads (0% mode mixity corresponding to pure normal loading and 100% to pure shear). The GMC model consisted of a doubly-periodic, square-packed RUC subjected to strain driven, cyclic loading (Figure. 4).

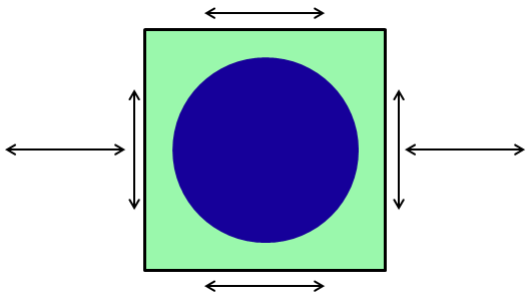

Figure. 4: A schematic representation of a fiber/matrix RUC subjected to combined normal and shear loading

The RUC was composed of 14 subcells x 14 subcells. A convergence study was conducted, and this architecture represented the least refined RUC that provided a converged solution. The fiber volume fraction of the RUC was 60% for both the FEM and GMC models. Since the debonding formulation uses energy release rates, it is important to use realistic dimensions for the RUC. Therefore a typical fiber radius of 5μm was chosen for both the FEM and GMC models. Similarly, the FEM model of the RUC, with user-defined cohesive elements (Naghipour, et al. [8]) placed at the fiber/matrix interface, was subjected to the same loading conditions. The degradation of the global transverse stress was monitored as number of cycles grew. The total amplitude of the displacement/strain-controlled cyclic loading was assumed to be 5e-4 mm. Convergence in the FEM simulation was achieved using a 75 element x 75 element mesh, which is computationally very costly, but necessary for achieving accurate results. The repeating nature of the fiber/matrix geometry is taken in to consideration via applying periodic boundary conditions in the FEM and GMC simulations (periodic boundary conditions are automatically assumed in the GMC formulation). It is worth mentioning that the same parameters for the matrix (epoxy 8552), fiber (carbon), and interface, obtained partially from available sources in literature and authors' previous experimental results [8], were used in GMC and the FEM simulation (see Table. 2).

Mechanical properties of epoxy 8552				
E_{11} (MPa)	ν_{12}	G_{12} (MPa)		
3450	0.35	1270		
Mechanical properties of fiber (Carbon AS4)				
E_{11} (GPa)	E_{22} (GPa)	ν_{12}	G_{12} (GPa)	G_{23} (GPa)
388.2	7.6	0.4	15	9
Properties of interface (UEL and GMC) C^{Paris} =0.0616 mm/cycle m^{Paris} =1.15 G_{th}= 0.001 mJ/ mm^2 Total G_c = 0.8 mJ/mm^2 ΔN=1 m=1				

Table 2: Properties used in GMC and FEM simulations for AS4/epoxy 8552

The user-developed cohesive element in FEM has been demonstrated the reliable and predictive capability to capture the cyclic delamination growth according to Naghipour et al. [8] and therefore was used as a validation tool. A comparison of the GMC and FEM results is presented in Figure. 5. Very good agreement of stress degradation in subsequent cycles was achieved, when comparing the fiber/matrix debonding in GMC with the corresponding FEM simulations (Figure. 5) for various normal/ shear combinations. The variation in results was higher for combined normal and shear loading cases, with a mean relative error value of 12%, compared to pure normal or pure shear loadings (mean relative error value of 5%). The interfacial debonding formulation incorporated a coupled, mixed-mode fracture energy evolution law. However, in GMC the normal and shear stresses are uncoupled; i.e., when a purely normal stress state is applied, only normal stresses will develop locally, and vice versa. Thus, under combined applied normal-shear loading cases, the error introduced by the lack of local normal-shear stress coupling is exacerbated when a mixed-mode fracture energy evolution law is utilized because the stresses that should arise due to coupling, and would contribute significantly to the overall degradation of the interface, are absent. Under pure normal or shear loading, the degradation due to the stresses arising from coupling is a second order effect.

However, the relatively low computational cost of the cyclic debonding analysis in GMC compensates for the mentioned modest error values. For the pure normal case the FEM runtime was 5300 seconds, whereas, the GMC solution was obtained in 180 seconds. On average, the GMC solution was 40 times faster than the FE solution. If fidelity is valued over efficiency, HFGMC can be employed at an added computational expense. The stress degradation calculated through GMC is higher compared to FE results for all loading cases, which shows the consistency of both solutions.

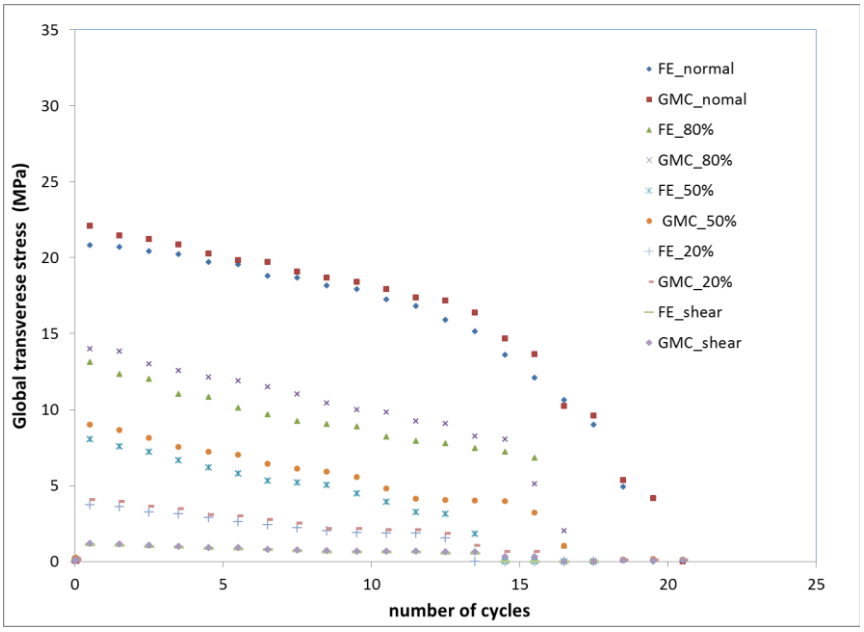

Figure. 5: Degradation of the global transverse stress versus number of cycles for different combinations of normal and shear modes (various mode mixities) comparison between FE and GMC result

After validating the reliability and predictive capability of the implemented cyclic debonding module in GMC via comparison to corresponding FEM simulations, cyclic debonding of the Sic fiber/ Ti-15-3 matrix was carried out in GMC using the above-mentioned RUC architecture and loading conditions (505 normal/shear mode mixity). Individual fiber and matrix properties are obtained partially from Authors' previous work [4] and from literature. A successive degradation of the stress versus number of cycles, however with a lower slope of degradation compared to the carbon/epoxy composite, is observed in this case too (Figure. 6).

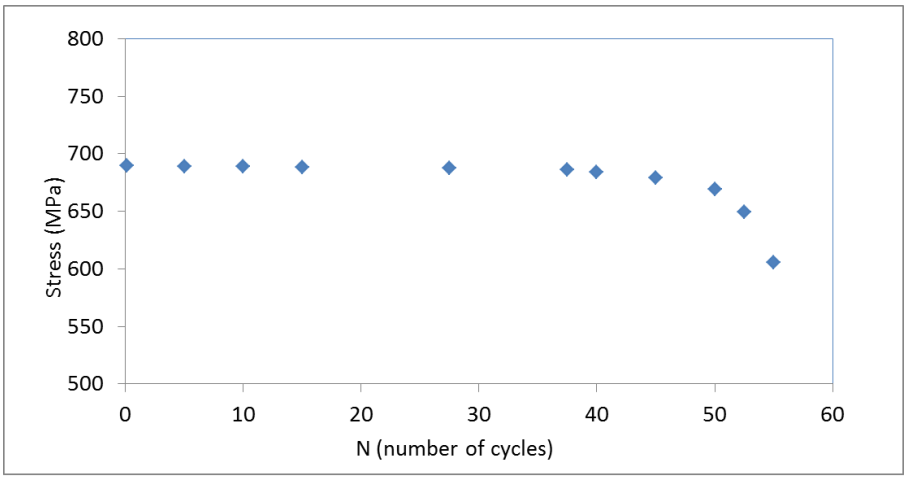

Figure. 6: Interfacial debonding stress degradation versus number of cycles (Ti15-3/Sic matrix/fiber)

Bednarcyk and Arnold [4] demonstrated that GMC is capable to model the static and cyclic failure response of SiC/Ti-15-3 laminates successfully, however without considering the cyclically debonding matrix/fiber interface. They used the above-described damage models for the fiber and matrix (except the cyclic debonding of interface), to predict the LCF life of $[\pm 30]_{2s}$ and $[\pm 45]_{2s}$ laminates, as well as the transverse $[90]_8$ composite at 427 °C within GMC. Detailed information on the model and used parameters can be found in Bednarcyk and Arnold [4]. The obtained results by the authors are re-demonstrated here in Figure. 6. It clearly demonstrates that the incorporated micro scale models of GMC successfully capture the experimental data [15,16] for this complex problem. For the $[\pm 30]_{2s}$ laminate, the agreement appears to be better in the higher life (low stress) range compared to the high stress range. Potential explanations for this discrepancy, given by Bednarcyk and Arnold [4], include increased fiber damage due to the off-axis fiber orientation and inaccuracy of the matrix stress field due GMC's lack of normal-shear coupling. In contrast to the $[\pm 30]_{2s}$, the $[90]_8$ composite displays a good agreement with experiment for the lower life range, but not for higher life range. The $[90]_8$ composite is dominated to the greatest extent by the matrix/matrix and interfacial cracking behavior, and thus this discrepancy most probably arises from interfacial cracking under cyclic loading. Not considering the interfacial cracking during successive cycles might cause GMC to overpredict the life of the $[90]_8$ composite as illustrated in Figure. 6. As a significant future scope, the newly developed (above-described) sub-model, which takes the successive cyclic evolution of interfacial cracking in to account, is supposed to improve the results for the$[90]_8$ laminate, once combined together with other sub-models in the laminate level.

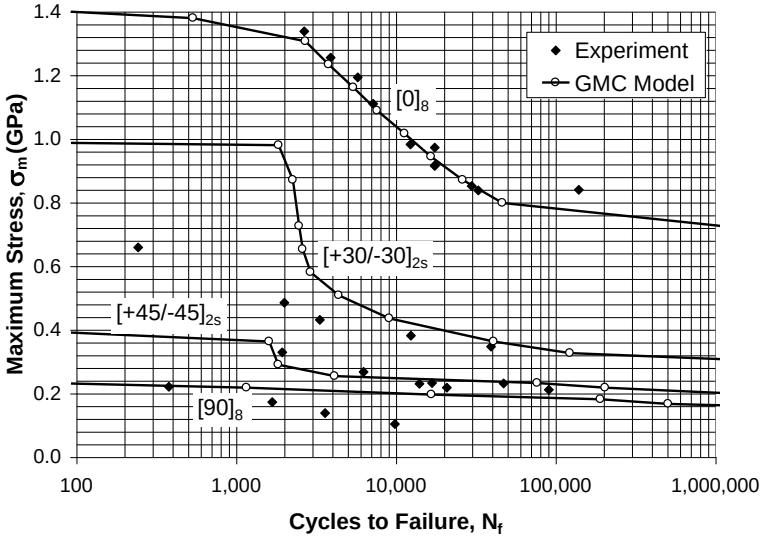

Figure. 6: Comparison of model LCF life predictions (S-N curves) with experiment for 35% SCS-6/Ti-15-3[4]

V. Conclusion

Simulation of debonding of the fiber/matrix interface due to cyclic loading, via implementation a fatigue crack growth law in to the available formulation of GMC, was accomplished, and the results were compared to a previously, experimentally validated fatigue delamination FE model. The stress degradation in subsequent cycles is captured with minimal error for pure cyclic normal/ shear loading cases when comparing the fiber/matrix debonding in GMC with the corresponding FE simulations. Later, the newly implemented GMC sub-model, which incorporates the successive cyclic degradation of fiber/matrix interface with a Paris-type fatigue law embedded in the interfacial debonding formulation, is supposed to improve the previously obtained results when use in parallel with the other sub-models.

References

[1]Aboudi, J., "Micromechanics of Composite Materials: A Unified Micromechanical Approach", Elsevier, Amsterdam, 1991.

[2]Aboudi, J., "Micromechanical Analysis of Thermo-Inelastic Multiphase Short-Fiber Composites", Composites Engineering Vol. 5, No. 7, 1995, pp. 839-850.

[3]Arnold, S.M., Bednarcyk, B.A., Wilt, T.E., Trowbridge, D., MAC/GMC User Guide: Version 3.0. NASA/TM-209070, 1999.

[4]Bednarcyk, B.A., Arnold, S.M., "Fully coupled micro/macro deformation, damage, and failure prediction for sic/ti-15-3 laminates", Journal of aerospace Engineering Vol. 15, 2002, pp. 74-83.

[5]Curtin, W.A., "Theory of Mechanical Properties of Ceramic-Matrix Composites", Journal of the American Ceramics Society Vol. 74, No. 11, 1991, pp. 2837-45.

[6]Bednarcyk, B.A., Arnold, S.M., "A New Local Failure Model With Application to the Longitudinal Tensile Behavior of Continuously Reinforced Titanium Composites". NASA/TM-210027, 2000.

[7]Arnold, S.M., Kruch, S., "Differential Continuum Damage Mechanics Models for Creep and Fatigue of Unidirectional Metal Matrix Composites", International Journal of Damage Mechanics 3 (2), 1994, pp. 170-191.

[8]Naghipour P, Bartsch M, Voggenreiter H, "Simulation and experimental validation of mixed mode delamination in multidirectional CF/PEEK laminates under fatigue loading", International Journal of Solids and structures Vol. 47, 2011, pp. 1070-1081.

[9]Mendelson, A., "Plasticity: Theory and Application", Krieger Publishing Co, 1983.

[10]Johnson, W.S., Lubowinski, S.J., Highsmith, A.L., "Mechanical Characterization of SCS-6/Ti-15-3 Metal Matrix Composites at Room Temperature. Thermal and Mechanical Behavior of Ceramic and Metal Matrix Composites", ASTM STP 1080, J.M. Kennedy, H.H. Moeller, and W.S. Johnson (Eds.), 1990, pp. 193-218.

[11]Mall, S. and Nicholas, T., "Titanium Matrix Composites, Mechanical Behavior", Technomic, 1998.

[12]Bednarcyk, B.A., Arnold, S.M., "Transverse Tensile and Creep Modeling of Continuously Reinforced Titanium Composites with Local Debonding", NASA/TM-210029, 2000.

[13]Jones, J.P., Whittier, J.S., 1967. "Waves at Flexibly Bonded Interfaces", Journal of Applied Mechanics Vol. 34, 1967, pp. 905-909

[14]Paris, P., Erdogan, F., "Critical analysis of propagation laws". J. Basic Eng, Vol. 85, 1963, pp. 528–534.
[15]Lerch, B.A., 1990. Fatigue Behavior of SiC/Ti-15-3 Laminates. HiTemp Review 1990, NASA CP 10051, pp. 35-1- 35-9.
[16]Lerch, B.A., Saltsman, J.F., 1993. Tensile Deformation of SiC/Ti-15-3 Laminates. Composite Materials: Fatigue B and Fracture, Fourth Volume, ASTM STP 1156, eds. W.W. Stinchcomb and N.E. Ashbaugh, ASTM, Philadelphia, pp. 161-175.